

Theory of optical imaging beyond the diffraction limit with a far-field superlens

Stéphane Durant,* Zhaowei Liu, Nicholas Fang,[†] and Xiang Zhang[‡]
 5130 Etcheverry Hall, NSF Nanoscale Science and Engineering Center (NSEC)
 University of California, Berkeley CA 94720-1740, USA
 (Dated: May 23rd 2005, last revision October 30, 2018)

Recent theoretical and experimental studies have shown that imaging with resolution well beyond the diffraction limit can be obtained with so-called superlenses. Images formed by such superlenses are, however, in the near field only, or a fraction of wavelength away from the lens. In this paper, we propose a far-field superlens (FSL) device which is composed of a planar superlens with periodical corrugation. We show in theory that when an object is placed in close proximity of such a FSL, a unique image can be formed in far-field. As an example, we demonstrate numerically that images of 40 nm lines with a 30 nm gap can be obtained from far-field data with properly designed FSL working at 376nm wavelength.

PACS numbers: 78.66.-w, 42.30.Lr, 78.66.Bz, 73.20.Mf

I. INTRODUCTION

Conventional optical lens imaging suffers from the diffraction limit which originates from the loss of evanescent waves that cannot travel to the far field. In the near-field, an object under illumination scatters both propagating and evanescent waves. Propagating waves carry the low spatial resolution information on the field modulation up to λ_0/n , where λ_0 is the illumination wavelength in vacuum and n is the refractive index of the surrounding medium. On the other hand, information on modulation of the field smaller than λ_0/n are carried by evanescent waves.

One promising approach of imaging beyond the diffraction limit emerged with the recent proposal of superlenses[1]. Basically a superlens is made of a slab of material that can support surface waves along the slab from electromagnetic excitation. In contrast with conventional material for which evanescent waves decays, using a superlens, evanescent waves can be transmitted with enhanced amplitude resulting from the surface wave excitation. Therefore a superlens has the ability to effectively recover the evanescent components radiated by the object in the image plane[2][3]. A good image can be obtained if the enhancement of evanescent waves by the superlens occurs within a broadband of spatial frequency. A superlens can be constructed from metamaterial with effective negative index media[4][5] consisting of metallic resonators, and dielectric[6][7][8] or metallic[9] photonic crystals consisting of periodically varying dielectric material. Also a superlens can be built from a slab of natural material that can support surface wave polaritons[3][10][11] with either negative per-

mittivity or negative permeability. Experimental studies have demonstrated superlens imaging both in microwave regime[12] using a two dimensional photonic crystal and in optical regime using a silver film[3][13][14]. Although the resolution of the superlens is still limited by the internal absorption losses of the materials due to inherent in strongly dispersive material[15], imaging well beyond the diffraction limit has been shown.

However, there is one drawback to the planar superlens. The superlens images are still in near-field zone as demonstrated by Podolskiy et al.[16], since the enhanced evanescent waves remain evanescent after transmission and vanish very quickly outside the superlens. Therefore, a challenge remains as how to use the superlens effect to form an image in far field with a resolution beyond the diffraction limit.

Another approach to recover the evanescent waves is to introduce an antenna into the near field that interacts with the evanescent waves and then radiates into the far field. In fact, this is the fundamental principle of the near-field scanning optical microscopy (NSOM) where optical nanoantennas such as plasmonic nanoparticles or metallic tips are used. Considerable studies have been devoted to interpret the far-field signals[17][18][19][20][21] depending of the NSOM configuration, and images with resolution down to 10nm have been demonstrated possible. Nevertheless, NSOM do not project a physical image as a conventional lens does, and the slow scan speed prevents a dynamic imaging[22], often of practical importance.

In this letter, we show theoretically that a new device termed as *far-field superlens* (FSL) can overcome the near-field limitation of a superlens, that is, in other words, able to project in far-field, an image of the evanescent component of the near-field. Moreover, we demonstrate theoretically that the image is unique. The image pattern is not a real space image, but rather provides the field angular spectrum[23], i.e. information on the object in spatial spectral domain. The far-field signal can be easily processed numerically in order to obtain a real space image of the local field distribution above the ob-

*Electronic address: stephane.durant@gmail.com

[†]Present address Department of Mechanical and Industrial Engineering, University of Illinois at Urbana-Champaign 158 Mechanical Engineering Building, MC-244 1206 West Green Street Urbana, IL 61801

[‡]Electronic address: xiang@berkeley.edu

ject with a resolution beyond the diffraction limit. As an example, a realistic design of an optical FSL made of metal/dielectric is proposed from exact numerical calculation.

II. IMAGING THEORY WITH A FAR-FIELD SUPERLENS MADE OF ARBITRARY MATERIAL

Adding a periodic grating on a superlens positioned in the near-field above an object may help to realize a lens-like imaging with a resolution below the diffraction limit. However, the imaging capability of a grating is not straightforward. Let us first introduce some general transmission properties of a grating without considering the superlens effect. We assume an object radiating optical waves at a wavelength λ_0 below a grating immersed into the same medium with a refractive index n . For the sake of simplicity and without losing generality, we consider a 2 dimensional problem where the material properties of both object and grating are function of (x, z) and invariant along the y axis. The grating is periodic along the x axis with a periodicity d . Periodic gratings are known to be able to couple out evanescent waves into propagating waves by a simple diffraction process. This property can be understood by writing the for instance the grating law:

$$k' = k + pG, \quad (1)$$

where k' and k are the transmitted and the incident transverse wave number respectively; p is the diffraction order; and G is the grating wave number of the grating. The transverse wave number is the projection of the wavevector of a plane wave along the x axis. Transverse wave number of evanescent waves are such that $|k| > nk_0$ where $k_0 = 2\pi/\lambda_0$, while transverse wave number of propagating waves satisfy to $|k| < nk_0$. Incident evanescent waves with a large k can be lowered by the grating wave number using for instance the order $p = -1$ of diffraction. Evanescent waves can be converted by this way into propagating waves that reach the far-field if G is large enough. But incident propagating waves would be also transmitted in far-field through the order $p = 0$ without wave number change. So that incident propagating and evanescent waves transmitted through the order 0 and -1 respectively will overlap in far-field making it difficult to separate them for imaging purposes. Indeed, waves transmitted in far-field for instance with a transverse wave number $|k'| < nk_0$ are the results of the overlap of incident waves transmitted through several orders p with transverse wave numbers satisfying:

$$k_p = k' - pG. \quad (2)$$

Let us write the relationship between the field transmitted in far-field and the incident field assuming TM polarized waves where the magnetic field H is oriented

along the y axis. The H -field transmitted above the grating with and its angular spectrum[23] are noted $H_t(x, z)$ and $\tilde{H}_t(k', z)$. Only plane waves with $|k'| < nk_0$ that can reach the far-field are considered. The near field radiated by the object under the grating with $z_0 < z < z_1$ is noted $H_{obj}(x, z)$. The near-field can be decomposed into a broadband angular spectrum of both propagating ($|k| < nk_0$) and evanescent ($|k| > nk_0$) plane waves. Separated by a grating, those two angular spectra are linked by a discrete linear summation of waves scattered into all orders of diffraction:

$$\tilde{H}_t(k', z_2) = \sum_{p=-\infty}^{+\infty} t_p(k_p) \tilde{H}_{obj}(k_p, z_1), \quad (3)$$

In Eq. (3), t_p is the p -order field transfer function of the grating from $z = z_1$ to $z = z_2$, defined as the ratio between the field transmitted in the order p of diffraction, and the field of an incident plane wave. The transfer function is a convenient tool commonly used in Fourier optics[23] to describe the transmission properties of optical system by plane waves. Transfer functions can be either measured experimentally or numerically by solving Maxwell's equations.

In general, the original near-field $\tilde{H}_{obj}(k, z_1)$, cannot be retrieved unambiguously from the far-field measurement of the angular spectrum $\tilde{H}_t(k, z)$ using Eq. (2-3) because of an overlap of several incident plane waves with different k_p scattered into with the same transverse wave number k' (the same direction). In general, there is no one-to-one relationship between the near-field angular radiated by the object and the far-field angular spectrum transmitted by a grating.

We demonstrate that this problem of the overlap of waves transmitted through several order of diffraction can be overcome by combining the superlens effect to the diffraction properties of a grating. The imaging principles can be understood following a very simple picture. Let us look first at transmission properties of a planar superlens as show in Fig 1a. Transmitted amplitude of incident evanescent waves (in black) are substantially enhanced through the slab because of the superlens effect. Comparatively incident propagating waves are poorly transmitted (in red). However, after transmission enhanced evanescent waves remain evanescent, limiting imaging with a superlens in the near-field zone. In contrast, let us consider now transmission properties of planar superlens corrugated with a subwavelength periodic structure termed as *far-field superlens* (FSL). As shown in Fig. 1b, a FSL not only enhances the incident evanescent field because of the excitation of surface waves in the slab based superlens, but also effectively convert these waves into propagating waves by scattering through a negative diffraction order of the grating following Eq 1. Overall, these incident evanescent waves transmitted and converted into propagating waves are projected in the far-field with large amplitude. In the others hand compared to the transmission of incident evanescent waves, inci-

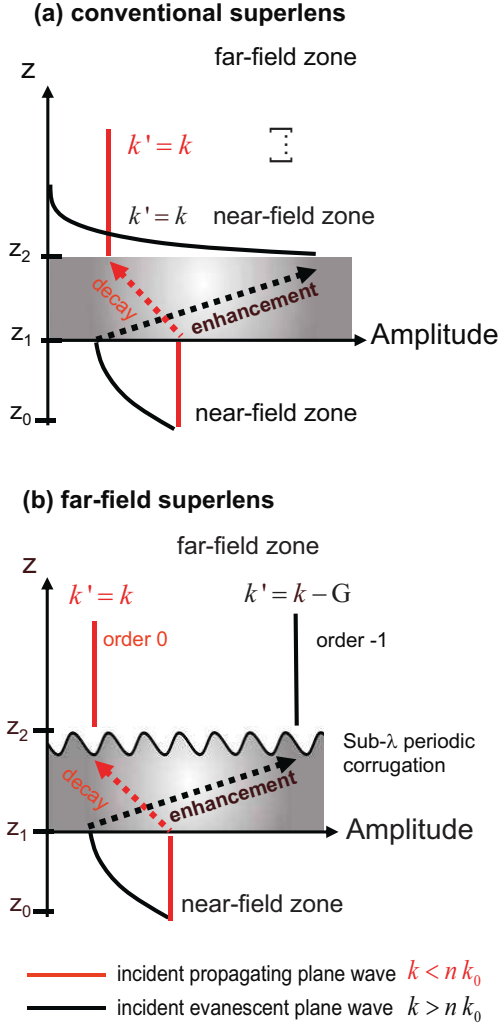


FIG. 1: Schematic picture of the transmission properties of a conventional superlens versus a far-field superlens. Through a conventional superlens (a), incident evanescent waves are enhanced in transmission and vanish quickly in the near-field zone. In contrast, a FSL (b) both enhances and converts them into propagating waves by diffraction while blocking incident propagating waves.

dent propagating waves are expected to be very poorly transmitted in far-field because of a lack of surface wave excitation, This property may be written:

$$|t_0(k - G)| \ll |t_{-1}(k)|, \quad (4)$$

with $|t_0(k - G)| \ll |t_{-1}(k)|$ within the bandwidth of evanescent waves for which the superlens effect occurs. Let us note that a similar relation occurs for negative transverse wave numbers if the grating has a -axis symmetry grating. If in addition, the superlens is designed with a large transmission within selective bandwidth $k \in [G; nk_0 + G]$, then the relationship between the far-field angular spectrum above the FSL and the near-field angular spectrum below the superlens given by Eq (2)

and (3) reduces to:

$$\tilde{H}_t(k', z_2) = t_{-1}(k) \tilde{H}_{obj}(k, z) \text{ where } k = k' + G, \quad (5)$$

for the positive half-space $0 < k' < nk_0$; and

$$\tilde{H}_t(k', z_1) = t_{+1}(k) \tilde{H}_{obj}(k, z) \text{ where } k = k' - G, \quad (6)$$

It follows from this result that any propagating wave transmitted in far-field by a FSL has a unique origin. For a positive k' for instance, the origin is the incident evanescent wave that has been transmitted through the diffraction order -1 with $k = k' + G$. This property is true for any k' so that there is a unique one to one relationship between the near-field angular spectrum under the FSL and the transmitted angular spectrum in far-field above the FSL. This results means that when an object is placed in close proximity of a FSL, a unique image of the near-field distribution can be projected in far-field. Moreover, using Eq. (5) and (6) and the rigorous diffraction theory[23], the near-field angular spectrum radiated by the object can be retrieved unambiguously from measurement of the far-field transmitted angular spectrum $\tilde{H}_t(k', z)$.

If both amplitude and phase of the angular spectrum can be measured in far-field, then a real space image of the near-field $\tilde{H}_{obj}(k, z)$ above the object can be reconstructed from $H_{obj}(x, z)$ using a simple inverse Fourier transform. However, the measurement of the phase is a practical difficulty. This difficulty appears also in diffraction optical microscopy[24] where both amplitude and phase of the angular spectrum have to be measured. For this purpose, an experimental set-up such as the one use by Lauer[24] based on interferometry may be a good approach. Alternatively, a direct real space image might be obtained using the Fourier transform transmission properties of lens[23] and other optical devices.

In principle, the maximum spatial frequency of the electromagnetic field that a FSL can image in far-field is $(n + \lambda_0/d)k_0$. Consequently, the best transverse resolution Δl that could be obtained on the image of the local density of electromagnetic energy is:

$$\Delta l = \frac{\lambda_0}{2(n + \lambda_0/d)}. \quad (7)$$

By comparison, the best resolution that could be achieved with a diffraction limited microscope is $\lambda_0/2n$ assuming a numerical aperture $NA=n$.

Using a FSL, we have demonstrated that the near-field angular spectrum and subsequently the local near-field distribution can be measured. However, the electromagnetic distribution of the field above the object depends on how the object is exposed. For instance, in normal incidence or with a grazing angle exposure by a plane wave, the FSL would provide accordingly different images. A model is needed if one wants to image an intrinsic property of the object that does not depend on the exposure condition such as the local polarizability or the local absorptivity.

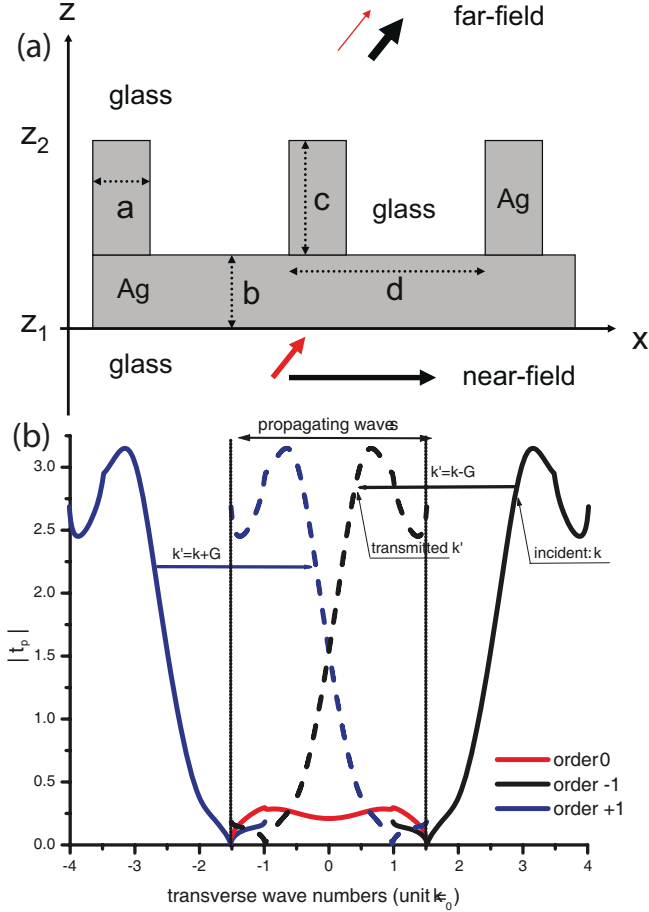


FIG. 2: (a) Design of an optical FSL working at $\lambda_0 = 376nm$ with $a = 45nm$; $b = 35nm$; $c = 55nm$; $d = 150nm$. (b) Amplitude of transmission factor through order $p = 0$ (red) and order $p = -1$ (black) from near-field $z = z_1$ to far-field ($z \gg \lambda_0$) of the optical FSL shown in (a). This FSL satisfies the requirement for imaging purpose: it provides a strong transmission of evanescent waves and convert them into propagating waves through the order -1 while the transmission of propagating waves through the order 0 is comparatively small.

III. CASE OF A SILVER FAR-FIELD SUPERLENS

How to design such a FSL for which the transmission properties satisfy to Eq (4) is a crucial question. One may start from the design of a superlens slab that enhances strongly incident evanescent waves within a large bandwidth. The enhancement can be provided by the excitation of surface waves mode of the slab based superlens. When a periodic corrugation is added on a superlens, the surface modes supported by the slab become leaky modes. As a result, as it was demonstrated by Smith et al[25] in case of a superlens made of metamaterial with a negative refractive index, corrugations at the interfaces of the superlens lead to smaller values of the enhancement of evanescent waves by the superlens. Despite this expected difficulty, we have successfully designed an

optical FSL made of silver/glass with the proper transfer functions satisfying to Eq (4), a necessary condition for imaging purpose. Details on the design of this FSL are provided in Ref.[26]. Feature sizes of this nanostructure are shown in Fig 2a. This FSL has been designed to work at $\lambda_0 = 376nm$ with TM polarized waves. We have computed the transfer functions of this structure from $z = z_1$ to the top $z = z_2$ by solving numerically Maxwell's equations using the Rigorous Coupled Wave Analysis (RCWA) algorithm[27][28] with experimental permittivity data of glass $\epsilon = 2.31$ and silver[29] $\epsilon = -3.16 + 0.2i$. The numerical solution provided has been tested using the theorem of reciprocity of electromagnetic waves and was applied for both propagating and evanescent waves[30][31]. The results of order 0 and ± 1 of the amplitude transfer functions are plotted in Fig. 2b. With a periodicity $d = 150nm$ and the wavelength $\lambda_0 = 376nm$, incident transverse wave numbers transmitted through the order -1 of the grating are shifted by $-2.5k_0$.

Fig. 2b clearly shows that Eq (4) is satisfied with $k \in [2.5; 4]k_0$, demonstrating that using a superlens periodically corrugated, a large bandwidth of evanescent waves can be both enhanced and converted into propagating waves with large amplitude, while incident propagating waves are poorly transmitted. Consequently, this FSL could be used for imaging with resolution well below the diffraction limit. Fig 2b shows similarly that $|t_0(k + G)| \ll |t_{+1}(k)|$ with $k \in [-4; -2.5]k_0$.

In a superlens made of silver, surface plasmon polaritons[32] (SPP) play a key role on the enhancement of evanescent waves [2][3][13]. At a metal/dielectric interface, SPP are surface waves resulting from the coupling between p-polarized electromagnetic waves and the induced collective excitation of free electrons in the metal. In a silver film superlens, the wavelength and the thickness are chosen so that SPP can be excited within a large bandwidth of transverse wave numbers[3][13]. How the optical FSL presented in this letter has been designed in close connection to SPP behavior, is detailed in Ref.[26].

Due to the position of the selective bandwidth of enhancement as shown Fig. 2b, waves transmitted into order -1 and $+1$ can be substantially overlapped with $k \in [-0.2; 0.2]$. For this reason, this small bandwidth has to be omitted from the measurement in order to retrieve the near-field angular spectrum unambiguously. Finally, it can be deduced using Eq (5) and (6) that the near field angular spectrum $\tilde{H}_{obj}(k, z)$ with $k \in [-4; -2.7] \cup [2.7; 4]k_0$ can be retrieved from the measurement of the far-field angular spectrum $\tilde{H}_t(k', z)$ with $k' \in [-1.5; -0.2] \cup [0.2; 1.5]k_0$. Because this specific FSL can resolve a transverse field modulation with a maximum spatial frequency $4k_0$, the transverse resolution on the image of the local density of electromagnetic energy is $\lambda_0/8$. By comparison, the resolution of diffraction limited microscope is $\lambda_0/3$ with a numerical aperture $NA = 1.5$.

As an example, we provide the result of the image reconstruction using a FSL, of an object constituted of

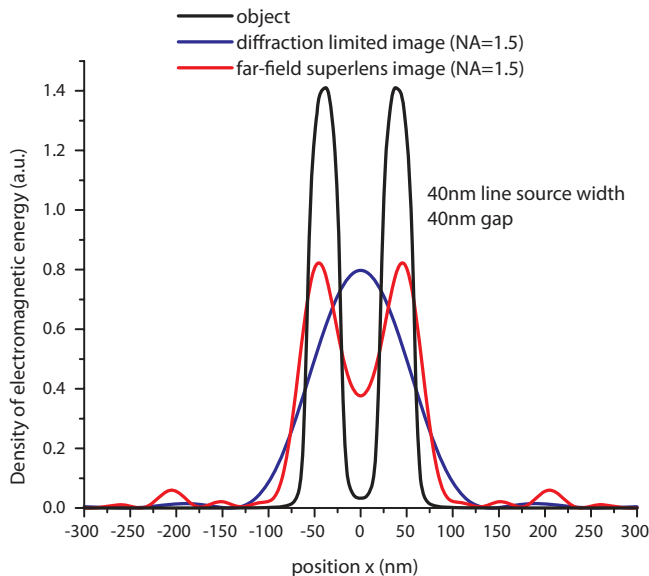


FIG. 3: Electromagnetic energy 5nm above the object and corresponding images with and without FSL assuming in both case a numerical aperture $NA=1.5$. Image of the density of electromagnetic energy with the FSL is reconstructed using Eq 5 and 6 and from the rigorous computation of the transmitted angular spectrum in far-field $z \gg \lambda_0$. This result computed rigorously directly demonstrates the optical imaging method with resolution below the diffraction limit from Far-field data, using a FSL made of silver/glass without any scanning

two 40nm lines sources of coherent TM waves separated by a deep subwavelength gap. A unity value of the H component is assumed on the two-line sources and vanished everywhere else. The near field computed at 5nm above the object using rigorous diffraction theory[23], is shown as the black curve in Fig. 3. For comparison, the computed diffraction limited image using conventional optical microscope assuming a numerical aperture $NA = 1.5$ is shown in blue in Fig 3. The optical FSL described in Fig 2a is placed 20nm above the object. The angular spectrum $\tilde{H}_t(k', z)$ transmitted by the FSL in far-field ($z \gg \lambda_0$) is computed rigorously using RCWA and Eq. (2-3). Values of $\tilde{H}_t(k', z)$ provide a complete set of data simulating a measured signals in an experiment. These known data are used subsequently for the image reconstruction. Because the designed silver FSL processes a unique one to one $k' \rightarrow k$ relation, it allows us to use this "experimental" data to retrieve the angular spectrum of the near-field 5nm above the object unambiguously only by using Eq.(5-6) and the rigorous diffraction theory. By combining this angular spectrum with its propagating component, we obtain the near-field angular spectrum 5nm above the object with $k \in [-4; -2.7] \cup [-1.5; 1.5] \cup [2.7; 4]k_0$. By applying a simple inverse Fourier transform, we finally obtain successively a reconstruction of the H -field distribution and

the image of the density of electromagnetic energy 5nm above the object. We have successively obtained faithful images reconstruction from 120nm down to 30nm gap. The case of 40nm gap is reported by the red curve in Fig. 3 where the separation of the two lines source is very clear. Let us note the formation of some artefacts[26] in the image may appear because of the missing band in the near-field angular spectrum. The image in case of 30nm gap (not shown) is the smallest gap between sources that we have been able to demonstrate following the Rayleigh criterion[33].

IV. CONCLUSION

We have demonstrated theoretically how to overcome the limitation of a conventional superlens for which only images in the near-field can be obtained[3][16]. We have shown that when the object is positioned close to a new device termed as the far-field superlens (FSL), a unique image of evanescent waves radiated by the object can be formed in far-field. In contrast to conventional near-field scanning optical microscope (NSOM), the FSL does not require scanning. In this sense, a FSL is similar with conventional lenses imaging with which a whole and unique image of an object can be recorded in a single snap-shot. From the measurement of the far-field image pattern and a simple inversion of the linear and scalar Eqs. (5) and (6), the near-field electromagnetic distribution above the object can be obtained with a resolution beyond the diffraction limit. By combining the superlens effect and the diffraction modes of a grating, the unique transmission properties of a FSL lies in a broadband excitation of surface wave leaky modes used to convert the incident near-field angular spectrum into a transmitted far-field angular spectrum, related by a one to one relationship. A realistic design of an optical FSL was given made of silver/glass with such a transmission properties, owing to the excitation of surface plasmon polariton (SPP) leaky modes. This new imaging approach has the potential to reach similar or better resolution than NSOM after more development. Such a far field superlens could have great impact not only in nano-scale imaging but also in nanolithography and photonic devices.

Acknowledgments

We are very grateful to Dr Q.-H. Wei for the critical reading of the manuscript. This research was supported by NSF Nano-scale Science and Engineering Center (DMI-0327077) and ONR/DARPA Multidisciplinary University Research Initiative (MURI) (Grant#N00014-01-1-0803).

-
- [1] J. B. Pendry, Phys. Rev. Lett. **85**, 183966 (2000).
- [2] D. R. Smith, Science **308**, 502 (2005).
- [3] N. Fang, H. Lee, C. Sun, and X. Zhang, Science **308**, 534 (2005).
- [4] V. Vesalogo, Sov. Phys. Usp. **10**, 509 (1968).
- [5] R. Shelby, D. Smith, and S. Schultz, Science **292**, 77 (2001).
- [6] C. Luo, S. Johnson, and J. Joannopoulos, Phys. Rev B **68**, 045115 (2003).
- [7] E. Cubukcu, K. Aydin, E. Ozbay, S. Foteinopolou, and C. Soukoulis, Phys. Rev. Lett. **91**, 207401 (2003).
- [8] C. Luo, S. Johnson, J. Joannopoulos, and J. Pendry, Phys. Rev. B **65**, 201104 (2002).
- [9] C. Luo, S. Johnson, J. Joannopoulos, and J. Pendry, Optics Express **11**, 746 (2003).
- [10] I. Larkin and M. Stockman, Nano Lett. **5**, 339 (2005).
- [11] V. Shalaev, W. Cai, U. Chettiar, H.-K. Yuan, A. Sarychev, V. Drachev, and A. Kildishev, Opt. lett. **30**, 3356 (2005).
- [12] P. Parimi, W. Lu, P. Vodo, and S. Sridhar, Nature (London) **426**, 404 (2002).
- [13] H. Lee, Y. Xiong, N. Fang, W. Srituravanich, S. Durant, M. Ambati, C. Sun, and X. Zhang, New J. of Phys. **7-255** (2005).
- [14] D. Melville and R. Blaikie, Opt. Express **13**, 2127 (2005).
- [15] N. Garcia and M. Nieto-Vesperinas, Phys. Rev. Lett. **11**, 746 (2002).
- [16] V. Podolskiy and E. Narimanov, Opt. Lett. **30**, 76 (2005).
- [17] J.-J. Greffet and R. Carminati, Progress in Surface Science **56**, 133 (1997).
- [18] R. Carminati and J.-J. Sáenz, Phys. Rev. Lett. **84**, 5156 (2000).
- [19] J.-J. Greffet, A. Sentenac, and R. Carminati, Optics Communications **116**, 20 (1995).
- [20] J. Porto, R. Carminati, and J.-J. Greffet, J. Appl. Phys. **88**, 4845 (2000).
- [21] P. Carney and *et al*, Phys. Rev. Lett. **92**, 163903 (2004).
- [22] B. Hetch, B. Sick, U. Wild, V. Deckert, R. Zenobi, O. Martin, and D. Pohl, J. Chem. Phys. **112**, 7761 (2000).
- [23] J. Goodman (McGraw-Hill, New York, 1996), 2nd ed.
- [24] V. Lauer, J. of Microsc. **205**, 165 (2001).
- [25] D. R. Smith, D. Schurig, M. Rosenbluth, S. Schultz, S. Ramakrishna, and J. Pendry, App. Phys. Lett **82**, 1506 (2003).
- [26] S. Durant, Z. Liu, J. Steele, and X. Zhang, JOSA B (in press) **23** (2006).
- [27] M. Moharam, E. Grann, D. Pommet, and T. Gaylord, JOSA A **12**, 1068 (1995).
- [28] M. Moharam, D. Pommet, E. Grann, and T. Gaylord, JOSA A **12**, 1077 (1995).
- [29] P. Johnson and R. Christy, Phys Rev. B **6**, 4370 (1972).
- [30] R. Carminati, J. Saenz, J.-J. Greffet, and M. Nieto-Vesperinas, Phys. Rev A **62**, 012712 (1998).
- [31] R. Carminati, M. Nieto-Vesperinas, and J.-J. Greffet, JOSA A **15**, 706 (1998).
- [32] W. Barnes, A. Dereux, and W. Ebbesen, Nature (London) **424**, 824 (2003).
- [33] M. Born and E. Wolf (Pergamon Press, New York, 1980), 6th ed.